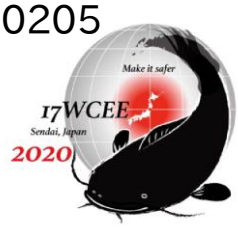

17th World Conference on Earthquake Engineering, 17WCEE
Sendai, Japan - September 13th to 18th 2020

SHAKE TABLE TEST OF A FULL-SCALE LOW-DAMAGE CONCRETE WALL BUILDING

Y. Lu [1], R. S. Henry [2], Y. Zhou [3], G. W. Rodgers [4], K. Elwood [5], A. Gu [6] and T. Y. Yang [7]

[1] Research Fellow, University of Auckland, Auckland, New Zealand, yiqiu.lu@auckland.ac.nz
[2] Senior lecturer, University of Auckland, Auckland, New Zealand, rs.henry@auckland.ac.nz
[3] Professor, Tongji University, Shanghai, China, yingzhou@tongji.edu.cn
[4] Professor, University of Canterbury, Christchurch, New Zealand, geoff.rodgers@canterbury.ac.nz
[5] Professor, University of Auckland, Auckland, New Zealand, k.elwood@auckland.ac.nz
[6] PhD candidate, Tongji University, Shanghai, China, 1296688048@qq.com
[7] Professor, Tongji University, Shanghai, China, yang@ilee-tj.com

Abstract

The increasing need to reduce damage and downtime of modern buildings has led to the development of a low-damage design philosophy, where earthquake demands can be safely resisted with damage confined to easily replaceable components. To provide essential evidence to support the development of low-damage concrete structures, a system level shake-table test was conducted on a full-scale low-damage concrete wall building implementing state-of-art design concepts. The building was tested on the multi-functional shake-table array at Tongji University as part of an ILEE-QuakeCoRE international collaborative research project. The 2-storey test building was designed with post-tensioned (PT) walls that provide the primary lateral-load resistance in both directions and a frame that utilised slotted beam connections. A number of alternative energy dissipation devices were also installed at wall base or/and beam-column joints of the building, including yielding steel fuses, lead-extrusion dampers, and non-linear viscous dampers. The building was subjected to 39 tests with a range of intensity ground motions, incorporating both unidirectional and bi-directional testing on the structure with different combinations of wall strength and energy dissipating devices. The 360 channels of test data has provided a significant dataset to verify design procedures, detailing practice, and numerical models. The building performed exceptionally well during the intense series of tests, indicating the new post-tensioned concrete wall buildings are a successful low-damage building solution. An overview of the key test results are presented, including the overall building response, performance of the PT walls, frames and wall-to-floor connections.

Keywords: Shake table test; reinforced concrete; low-damage; post-tensioning wall; slotted beam.

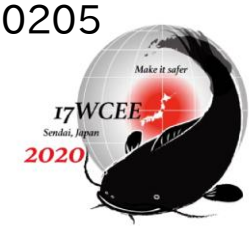

1. Introduction

The damage caused to conventional modern buildings during major earthquakes often leaves them requiring either costly repairs or demolition, as highlighted by the 2010/2011 Canterbury earthquakes in New Zealand [1, 2]. The increasing need to reduce damage and downtime to buildings following major earthquakes has led to the development of low-damage design philosophy, where the earthquake demands can be safely resisted with damage confined to replaceable components.

Post-tensioned (PT) concrete structural systems have been well developed using precast concrete components and concentrating plastic demands at easily replaceable energy dissipating elements [3]. Unboned PT wall systems consist of a precast concrete panel with unbonded PT tendons anchored between the top of the wall and the foundation. Previous research on PT walls has mostly focused on individual components and does not account for the complex interactions that can occur in real buildings during earthquakes [4-6]. However, evidence from recent research has indicated that these interactions can violate design assumptions and influence seismic behavior and capacity [7-10]. Dynamic building tests are required to understand the system level response and verify the new concepts of wall, floor, and frame systems, as well as wall-to-floor connections.

To verify the seismic response of a low-damage concrete wall building implementing state-of-art design concepts and practical construction details, a joint research project was proposed between the New Zealand Centre for Earthquake Resilience (QuakeCoRE) and the International Joint Research Laboratory of Earthquake Engineering (ILEE) in China. The project focused on a shake-table test of a two-storey PT wall building that incorporated design and detailing lessons from implemented buildings in New Zealand. The building was tested at the ILEE multi-functional shake-table array located at the Jiading campus of Tongji University. Both the global and local response of the building were monitored by a dense array of sensors during testing. The test results have allowed for a significant improvement in the understanding of the system-level behaviour of PT wall building during earthquakes. A summary of the test program and preliminary test results are presented, including the overall building response, performance of the PT walls, frames and wall-to-floor connections.

2. Test Program

2.1 Test building

The building was designed using the Direct Displacement-Based Design method [11], assuming the building is to be used for general office purposes and located in Wellington, New Zealand. The two-storey test building had plan dimensions of 5.4 × 8.95 m. The total height of the building from foundation surface was 8 m with each storey 4 m high. The building weighed roughly 1350 kN, close of the payload capacity of the shake table. The building structural system consisted of a perimeter frame and two exterior PT walls in both directions. The four PT walls were designed to primarily resist seismic loads in both directions. The perimeter frame was designed to primarily carry gravity loads and used a slotted beam detail [12]. The Level 1 floor system consisted of a long-span precast concrete double tee and a steel tray composite floor was used for level 2 in a short span configuration with a secondary steel beam aligned through the longitudinal center of the floor. The constructed building and the floor plan of the building are shown in Fig. 1 and Fig. 2, respectively. The building used detailing consistent with that implemented in buildings in New Zealand. The building design is described in detail by Lu et al. [13]. Key features included:

- Two alternative wall base details, consisting of a grouted joint detail with no shear dowels in the long-span direction and a recessed steel pocket detail in the short-span direction.
- Two alternative wall armouring approaches, consisting of a small steel angle in the long-span direction and a larger armoured end toe region in the short-span direction.

- Three alternative wall-to-floor connection approaches, consisting of a flexible link slab on level 1 of the long-span direction, flexible composite floor on level 2 of the long-span direction, and isolated steel tongue connection on both levels in the short-span direction.
- The building was designed for three lateral drift targets with different wall strength and energy dissipating devices, as summarised in Table 1. Various combinations of dissipating devises were installed at both the wall based and slotted beam joints, including steel fuses [14], HF2V lead dampers [15] and non-linear viscous dampers.

Fig. 1 - The test building on the shake-table array at Tongji University's Jiading campus

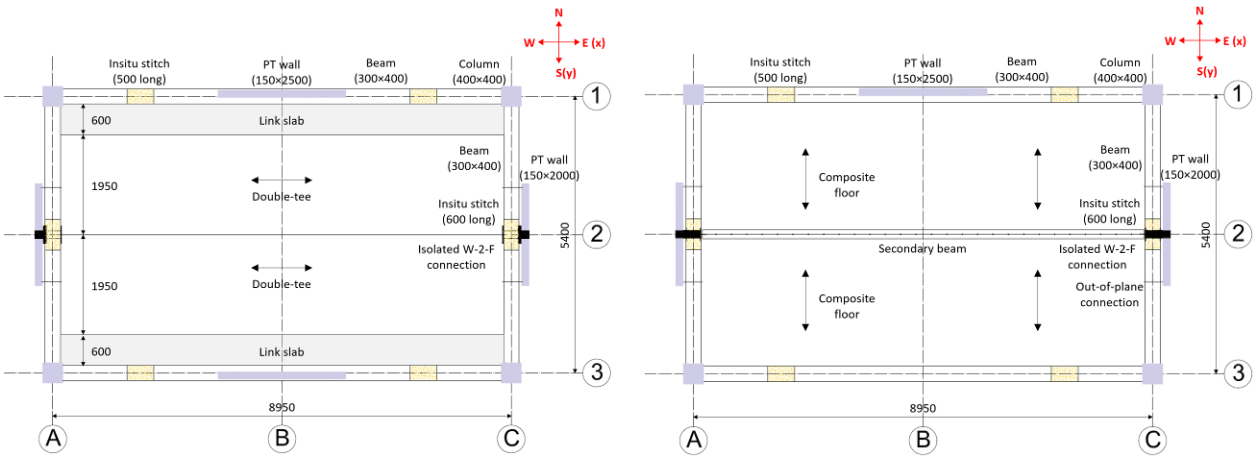

(a) Level 1 - Plan (b) Level 2 – Plan

Fig. 2 - Floor plans of the building

Table 1 - Design configurations of the test building

Design	Design drift	Dissipating devices	
		Wall base	Beam-column
1a	1%	Steel fuse	Steel fuse
1b	1%	Viscous damper	HF2V
1c	1%	Steel fuse	HF2V
2	2%	Steel fuse	N/A
3	3%	N/A	

2.2 Ground motions and test sequences

All the input ground motions included scaled components in two horizontal axes (X and Y). The input ground motion to simulate Serviceability Limit State (SLS) level earthquakes was from the Parachute Test Site station recorded during the 1979 Imperial Valley earthquake (RSN-187). The ground motions recorded from the Nishi-Akashi station during the 1995 Kobe earthquake (RSN-1111) and Saratoga – Aloha Ave station during the 1989 Loma Prieta earthquake (RSN-802) were selected to simulate design level Far-Fault (FF) and Near-Fault (NF) earthquakes, respectively. The Maximum Considered Earthquake (MCE) used same ground motions that simulated Design-Based Earthquakes (DBE) but with a larger scale factor. Finally, a long-duration ground motion that was recorded at the Sanfernando station during 1985 Chile earthquake (Chile) was selected to investigate the behaviour of the building subjected to a long-duration MCE event. The elastic 5% damped acceleration and displacement response spectra of the three input motions and the target response spectra for NZS 1170.5 SLS (25%), DBE and MCE in the location of Soil C in Wellington are compared in Fig. 3.

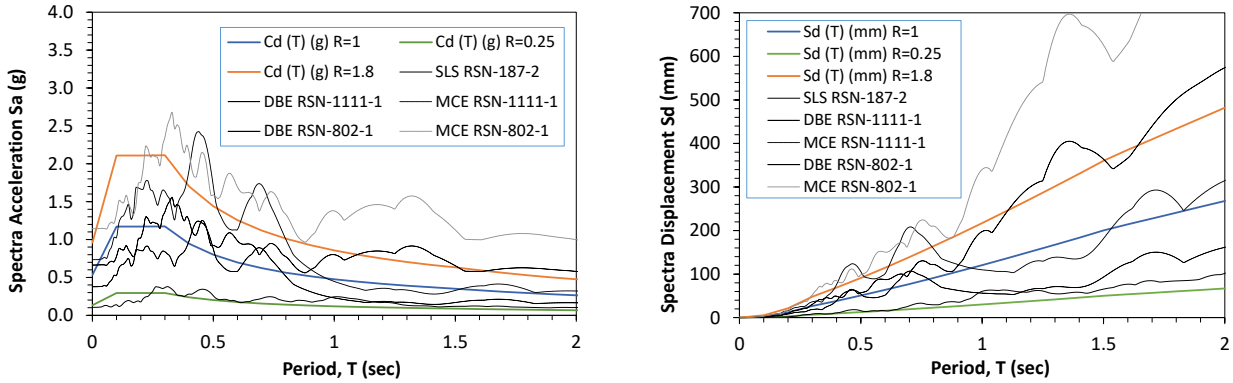

(a) Acceleration spectra (b) Displacement spectra

Fig. 3 - Response spectra comparison

Table 2 summarises the test sequence that was conducted over a period of 6 days. The building was subjected to 39 separate ground motions, consisting of five structural design configurations with different energy dissipating devices and combinations of ground motions including an SLS record, far field and a near fault DBE records, and short and long duration MCE records. The structure was subjected to unidirectional shaking in both axes of the building as well as bi-directional horizontal shaking. The building was first subjected to earthquakes in order of SLS (25%), repairable level (50%) and DBE (100%) for Design 1a, followed by DBE level of Design 1b and 1c. For Design 2, the building was subjected to DBE and MCE (180%) records, including the long-duration earthquake. In addition, the Design 2 configuration was modified to create deliberate eccentricities in wall strength to generate a torsional response, listed as 2T in Table 2. The final test (Design 3) was conducted with no dissipaters to test the resilience of the system after all of the dissipaters have failed and to induce maximum drift to the building to investigate the wall-to-floor interaction and potential damage.

2.3 Instrumentation

The test building was instrumented with 42 accelerometers, 96 string-pot displacement gauges, 159 linear-pot displacement gauges, 14 load cells, 8 load pins and 43 strain gauges to monitor the overall response of the test building as well as local component responses. The instrumentation recorded accelerations at different locations and levels in three components, global lateral displacements, uplifts of the column and wall bases, gap opening at the slotted beam joints, out-of-plane floor deflections at both levels, responses of the wall-to-floor connections, forces in the PT bars, elongations of the beams, concrete strains at wall toes, reinforcement strains at beam-column joints and floors, potential in-plane and out-of-plane slip at all the wall bases, rotations of double-tee and secondary beam, potential beam torsional rotations, and potential vertical and horizontal slip at the foundation-to-shake table joints.

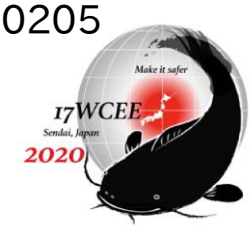

Table 2 - Test sequences

Day	Test #	Design	Intensity (Ru)	Ground motion	Direction
1	1-3	1a	25%	SLS (RSN - 187)	x, y, xy
2	4-6		50%	SLS (RSN - 187)	x, y, xy
	7-10		100%	DBE-FF (RSN - 1111)	x, y, xy
	11		25%	SLS (RSN - 187)	xy
	15	1c	100%	DBE-NF (RSN - 802)	xy
	16-18, 20	1b		DBE-FF (RSN - 1111)	x, y, xy
	19			DBE-NF (RSN - 802)	xy
4	21-23	2	100%	DBE-FF (RSN - 1111)	x, y, xy
	24			DBE-NF (RSN - 802)	xy
5	25-27		180%	MCE-FF (RSN = 802)	x, y, xy
	28		100%	MCE-L (Chile)	xy
	29		180%		x
6	30-33	2T	100%	DBE-FF (RSN - 1111)	y, xy
	34-35			DBE-NF (RSN - 802)	y, xy
	36	3	100%	DBE-FF (RSN - 1111)	xy
	37		120%	MCE-FF (RSN - 1111)	xy
	38		100%	MCE-FF (RSN - 1111)	x
	39		150%	MCE-FF (RSN - 1111)	x

3. Test Results

Overall, the test building performed extremely well, withstanding repeated tests at both design and maximum considered earthquake intensities with only minor damage to the wall toes and minor cracking to the floor slabs. Preliminary results from the overall building response as well as the performance of PT walls, frames and floors are summarised.

3.1 Overall Building response

Fig. 4 shows the lateral displacement profiles over the height of the building at peak drifts for Design 1a, Design 2 and Design 3 during bi-directional ground motions at different intensities. The displacements plotted in Fig. 4 is the center displacements at two orthogonal directions calculated as the average of the measurements of four corners, as shown in Fig. 5.

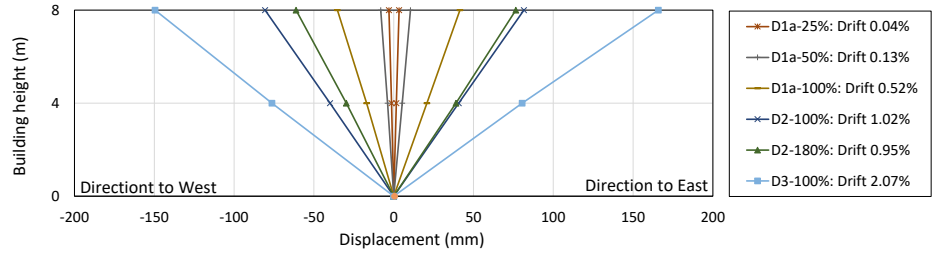

(a) x direction

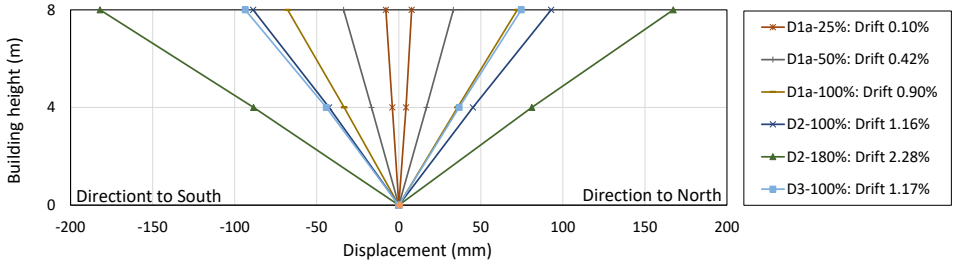

(b) y direction

Fig. 4 – Displacement profile of the test building at peak drift

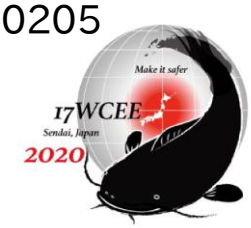

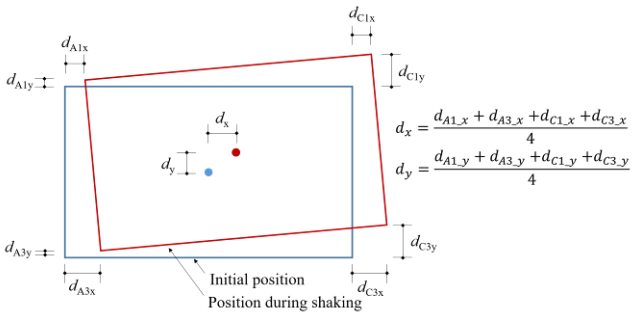

Fig. 5 – Illustration of calculation of building displacement

As shown in Fig. 4, the lateral displacement profiles are almost linear, confirming that the building response was controlled by near-rigid body rotation of PT walls. For all the cases, the peak drifts were smaller than the design drifts. For example, the peak drift to the North for Design 1a at 100% intensity was only 0.52%, approximately half of the design drift of 1.0%. The small drift was attributed to the overstrength of the building due to a combination of the safety factors induced in the DDBD design and the influence of wall-to-floor interactions. For most cases, the peak drift in the y direction was larger than in the the x direction as an isolated wall-to-floor connection was used in the y direction and so the overstrength due to wall-to-floor interaction was less significant. It should be noted that the peak drift in the y direction was smaller than x direction for Design 3. This larger drift in the x direction was attributed to the larger damage to the corners of wall 1 and 3 due to the minimal armouring and larger number of tests in the x direction. The building was significantly more flexible in the x direction during the ground motions for Design 3.

An example of time history response for the level 2 drifts, base shears, and base moments for Design 1a in the x direction during 100% intensity are plotted in Fig. 6. Base shears were calculated as the sum of horizontal inertia forces over the two floors, with inertia forces at each level calculated by multiplying floor mass and floor acceleration measured from the accelerometer installed at center of the floor area. Base moments were computed as the sum over floor horizontal inertia forces multiplied by the corresponding floor height. As shown in Fig. 6, the peak drift, base shear and base moment occurred at the same instant of 8.23s. The peak base shear and base moment were significantly higher than the design values. The peak shear was ~550 kN, roughly 70% higher than the design base shear and the peak base moment was ~3400 kN.m, 60% higher than the design base moment, again confirming the overstrength of building. In addition, the residual drift at the conclusions of testing was negligible (less than 0.05%), confirming the re-centering capability of PT wall systems.

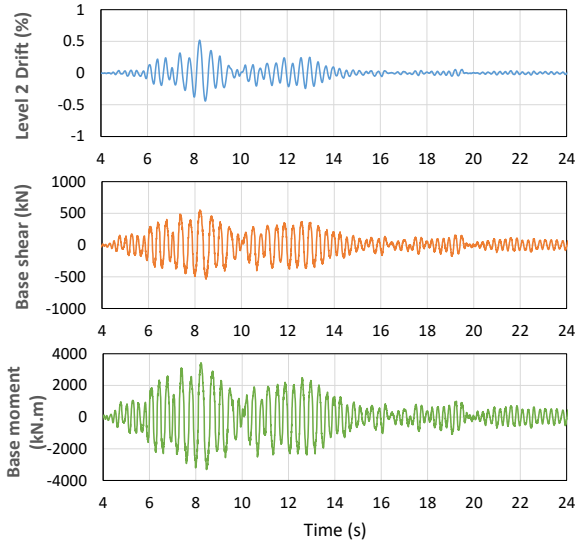

Fig. 6 – Response histories for the x direction of the Design 1a test building during 100% design intensity

3.2 Wall base

Two rows of linear-pot displacement gauges installed on each side of the wall base, respectively, allowed the gap-opening profiles and wall base rotations to be monitored. An example of uplifts along the length of wall 1 at peak drifts for Design 1a at 100% intensity are plotted in Fig. 7. The uplifts along the wall length were linear from both the northern and southern measurements. At the peak in-plane drift (to east), differences between the measurements on the north and south faces were negligible as the out-of-plane wall rotation was modest. However, the north and south face measurements at peak out-of-plane drifts for wall 1 were offset by around 2 mm, with a combination of in-plane and out-of-plane rotations resulted in a higher compressive strains in the corner of the wall.

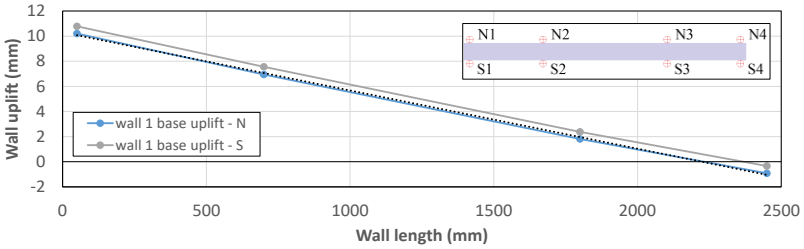

(a) wall uplift at peak drift to east

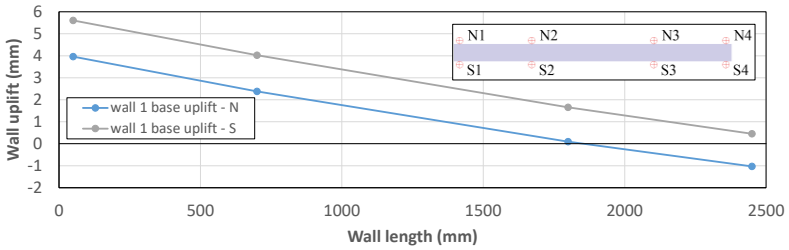

(b) wall uplift at peak drift to north

Fig. 7 - Uplift of wall 1 base at peak drift for Design 1a at 100% design intensity

Fig. 8 shows a plot of the time history wall base rotations for all four walls during the Design 1a 100% intensity test. The wall base rotation was calculated using the average measurement from north and south face linear-pot displacement gauges as shown in Eq. (1).

$$\theta = \frac{(u_{N1} - u_{N4}) + (u_{S1} - u_{S4})}{2l_w} \tag{1}$$

As shown in Fig. 8, the time history wall rotations are closely aligned to the global drift, again confirming that the majority of building lateral displacement was attributed to rocking of the PT wall. The peak wall rotation and peak global drift in the x direction were around 0.5% and occurred at the same instant of 8.23s, while the peak wall rotation and global drift in the y direction were 0.9% and occurred at 9.35s.

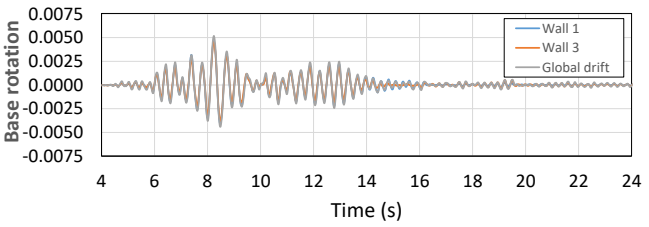

(a) wall 1 and 3

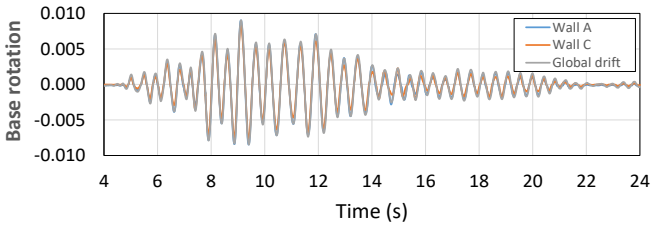

(b) wall A and C

Fig. 8 - Time history wall base rotations for Design 1a at 100% intensity

The two alternative wall base details performed well, with no significant wall sliding or out-of-plane walking. Fig. 9 shows examples of the final condition of the wall toes for wall 1 (conventional grouted

connection) and wall A (steel pocket connection). No spalling was observed at the wall toes following D1a-100% tests and only minor spalling occurred at the wall toes during larger intensity D2-100% and D2-180% tests.


(a) Wall 1 at Northeast corner


(b) Wall A at Southeast corner

Fig. 9 – Final condition of the PT wall bases

3.3 Frame

The frame performed well with only narrow cracks at the slotted beam joints and minor spalling during large intensity earthquakes. The column-to-foundation connection was designed to act as a pin. The connection used a rocking detail similar to PT walls. Gravity was relied on to prevent column uplift, but unstressed PT bars were also located in the column to provide additional uplift capacity during earthquakes. The columns behaved elastically as expected with no damage/cracks throughout all of the tests. Fig. 10 compares the time history column A1 base rotation versus global drift in the x direction for Design 1a at 100% intensity. The column base rotation and the drift match closely, indicating that the columns acted as a rigid body and the column bending or shear deformations were negligible. No spalling occurred at the column base and no damage occurred at the beam-column joints, as shown in Fig. 11.

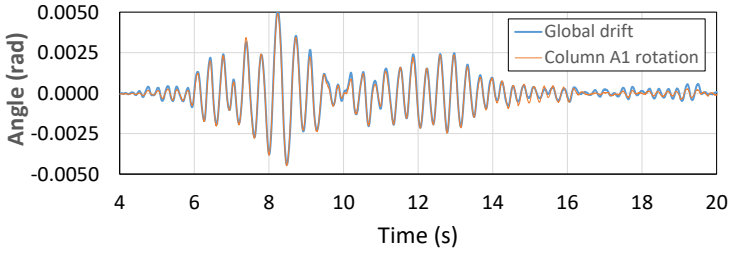

Fig. 10 – Comparison of time history column base rotation and global drift in the x direction for Design 1a at 100% design intensity

(a) Column base


(b) Column joint betweel L1 and L2

Fig. 11 - Final condition of column at end of testing

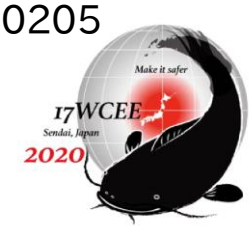

To overcome the shortcomings of traditional beam plastic hinges, slotted (non-tearing) beams were used at the frame joints. The inclusion of a slot adjacent to the column face allowed seismic rotations to be accommodated by opening and closing of the slot with rotation centered at the top of the beam. An example of time history beam-column rotation for Design 1a at 100% intensity for level 1 Beam 1 at Column A1 is plotted in Fig. 12 alongside the global drift in the x direction. It is interesting to note that the rotation and the global drift match closely for negative drifts while the beam joint rotation is slightly higher than the global drift for positive drifts. The inconsistency is due to the amplification of the beam rotation as the wall uplifts, as shown in Fig. 13.

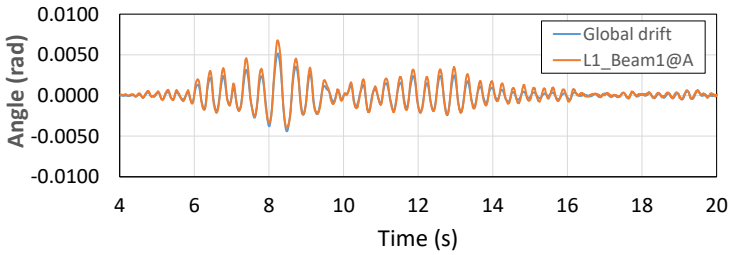

Fig. 12 - Comparison of time history slotted beam rotation and global drift in the x direction for Design 1a at 100% intensity

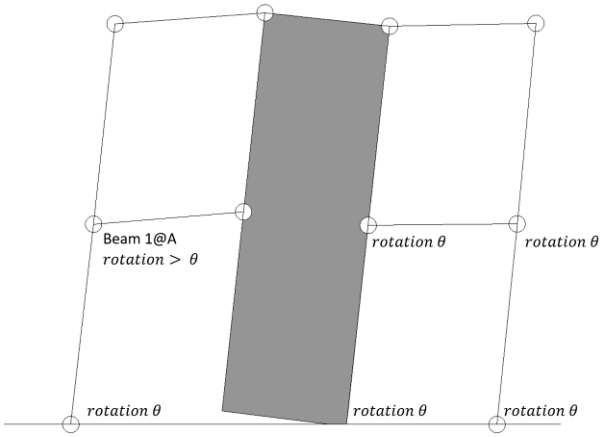

Fig. 13 - Illustration of slotted beam rotations

The slotted-beam connections performed well, minimising beam-elongation (frame dilation) demands on the floors and limiting residual crack widths. Fig. 14 shows examples of the final condition for the slotted beam joints. Only 1-2 diagonal cracks extended from the top of slot to the floor surface with maximum residual crack widths less than 1 mm.

(a) Beam A@1-L1 (b) Beam 1@Bc-L2

Fig. 14 - Slotted beam joint condition after different intensity earthquakes

3.4 Wall-to-floor interaction

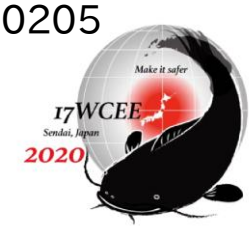

Out-of-plane floor deflections at different locations were measured by string-pot displacement gauges extending vertically from the shake-table to the bottom of the Level 1 floor and from the top of the Level 1 floor to the bottom of the Level 2 floor. The floor out-of-plane deformations were used to investigate the wall-to-floor interaction when different connections were implemented. An example, the level 1 floor deflections at peak drifts for Design 1a at 100% intensity are plotted in Fig. 15. The resulting floor deformations show how the wall picked up the edge of the floor and how this deformation was concentrated within the flexible link slab section. At the peak drift to the east, the vertical floor deformation near the West end of the wall was 7.4 mm larger than the floor deformation at the edge of the link slab near the double tees, and 10.3 mm larger than the floor deformation at column A. However, the flexible wall-to-floor connections used in the test building accommodated the wall deformations as intended, resulting in only minor cracks in the floors. Fig. 16 shows the crack maps of the entire Level 1 floor and an example of crack map photo of the link slab. As shown in Fig. 16, floor cracks were mainly concentrated within the two link slabs. The cracks were evenly distributed along the length of the link slab with a maximum residual crack width of approximately 1 mm.

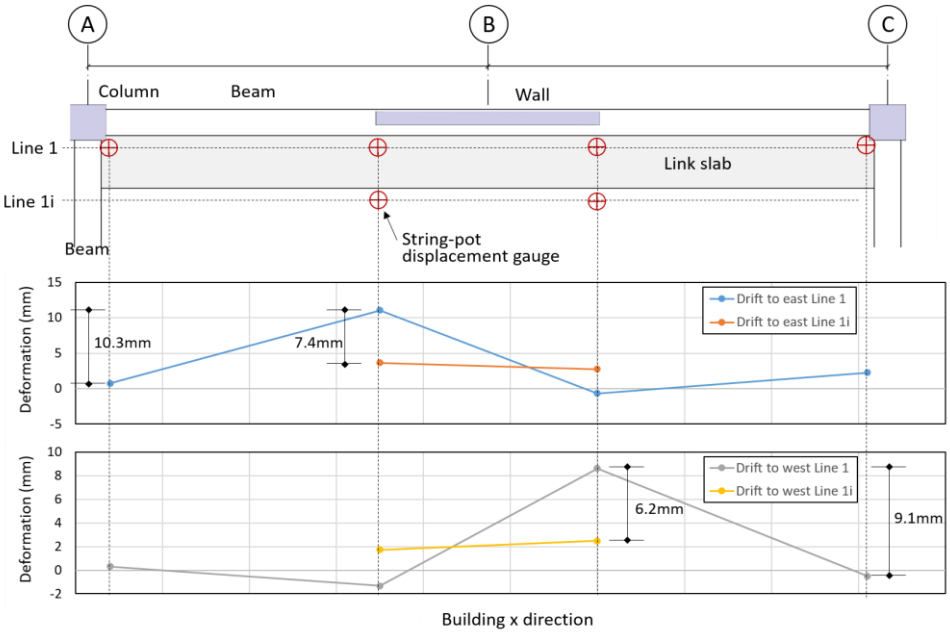

Fig. 15 – Link slab deflections at peak drift at x direction for Design 1a at 100% intensity

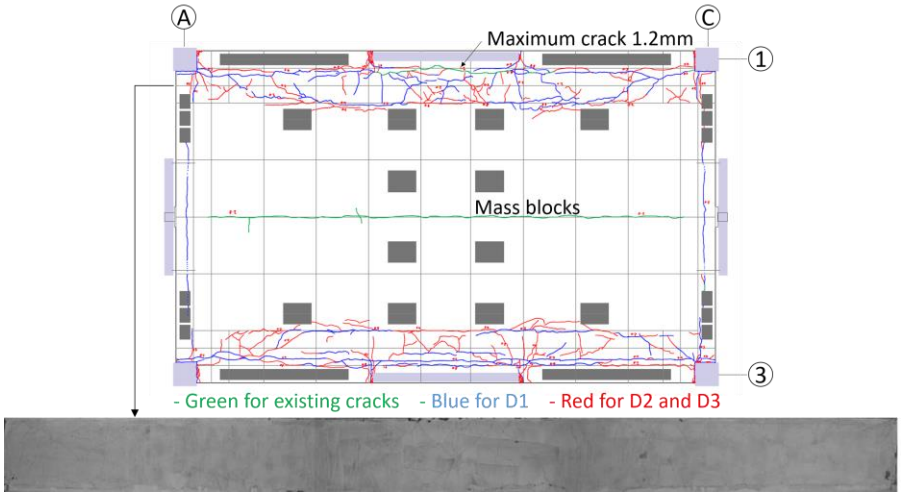

Fig. 16 – Crack map of link slab at end of test

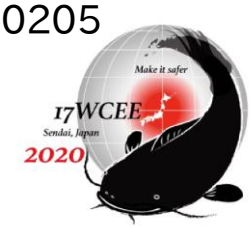

The isolated wall-to-floor connection was successful at preventing any unintended demand on the floor with no cracking observed around these connections. Fig. 17 shows an example of the final condition of the isolated wall-to-floor connection at Wall A, Level 2. The steel tongue performed well with only minor delamination and bending of the shims between the steel tongue and the armouring which could be easily improved with a better attachment method. The corresponding floor only had a minor cracks parallel to the wall along the interface between the beam and the floor. No cracks perpendicular to the wall length occurred around the isolated wall-to-floor connection.

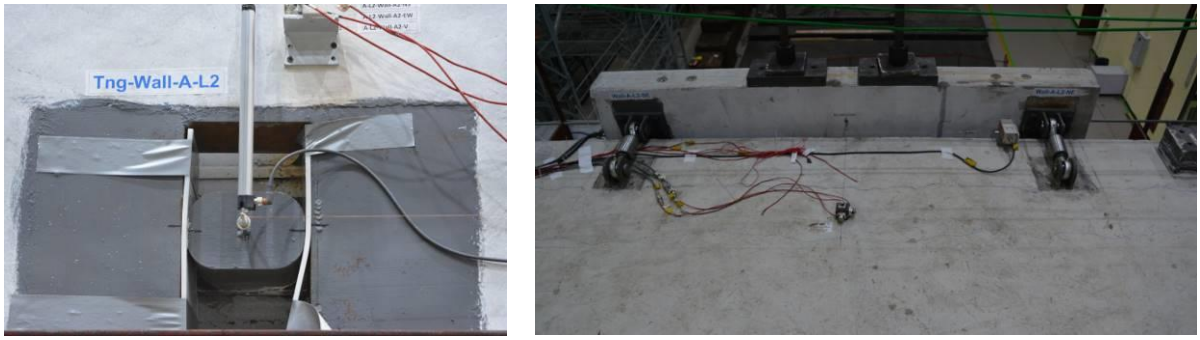

(a) Steel tongue (b) Floor

Fig. 17 - Final condition of the isolated wall-to-floor connection at Wall A level 2

4. Conclusions

The building performed well during the intense series of tests, providing confidence the new low-damage concrete buildings are an excellent low-damage building solution. The building exhibited only minor damage, with distributed cracking in the floors and cosmetic spalling in the wall toes that could be easily repaired. The building response was dominated by the rigid body rotation of the PT walls with almost linear displacement profiles over the height of the building. A significant overstrength was observed in the test building, resulted in the peak drifts during earthquakes being up to 50% less than the design drifts. The construction details used in the test building all performed extremely well. Both conventional grouted and steel pocketed wall-to-floor connections performed as intended with only minor spalling occurring at wall toes during large intensity earthquakes. In addition, the slotted beam joints accommodated the beam-column rotation and significantly reduced the potential damage at beam-column joints, without inducing any significant beam elongation or subsequent frame dilation. Finally, the flexible and isolated wall-to-floor connections were able to reduce and prevent unintended demand to the floor with only minor cracking observed.

5. Acknowledgements

The authors would like to acknowledge the funding provided by the International Joint Research Laboratory of Earthquake Engineering (ILEE) hosted at Tongji University, the Building Systems Performance branch of the New Zealand Ministry of Business, Innovation and Employment (MBIE), and the New Zealand Centre for Earthquake Resilience (QuakeCoRE). The advice and support from the project industry advisory group is also greatly appreciated, including Didier Pettinga, Alistair Cattanach, Tony Holden, Peter Smith, Des Bull, and Craig Muir. This project was (partially) supported by QuakeCoRE, a New Zealand Tertiary Education Commission-funded Centre. This is QuakeCoRE publication number 0554.

6. References

[1]. Kam WY, Pampanin S, and Elwood K (2011): Seismic performance of reinforced concrete buildings in the 22 February Christchurch (Lyttelton) earthquake. *Bulletin of the New Zealand Society for Earthquake Engineering*, **44**(4): 239-278.

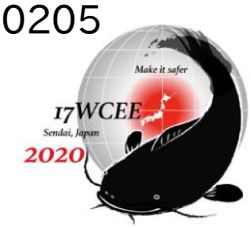

[2]. Canterbury Earthquakes Royal Commission (2012): Final report: Volume 2: The performance of Christchurch CBD buildings. http://canterbury.royalcommission.govt.nz/Commission-Reports. Wellington, New Zealand.

[3]. Priestley MJN, Sritharan SS, Conley JR, and Pampanin S (1999): Preliminary Results and Conclusions From the PRESSS Five-Story Precast Concrete Test Building. *PCI Journal*, **44**(6): 42-67.

[4]. Marriott D. (2009): The Development of High-Performance Post-Tensioned Rocking Systems for the Seismic Design of Structures. University of Canterbury, Doctor of Philosophy.

[5]. Twigden KM, Sritharan S, and Henry RS (2017): Cyclic testing of unbonded post-tensioned concrete wall systems with and without supplemental damping. *Engineering Structures*, **140**: 406-420.

[6]. Twigden KM and Henry RS (2019): Shake table testing of unbonded post-tensioned concrete walls with and without additional energy dissipation. *Soil Dynamics and Earthquake Engineering*, **119**: 375-389.

[7]. Henry RS, Aaleti S, Sritharan S, and Ingham JM (2012): Seismic analysis of a low-damage PREcast Wall with End Columns (PreWEC) including interaction with floor diaphragms. *SESOC Journal*, **25**(1).

[8]. Watkins J, Sritharan S, and Henry RS (2014). An experimental investigation of a wall-to-floor connector for self-centering walls. *Proceedings of the Tenth U.S. National Conference on Earthquake Engineering*. Anchorage, Alaska.

[9]. Liu Q, French C, Sritharan S, and Nakaki S (2015): Rocking Wall-Floor-Column Subassemblage Pseudo-Static Cyclic Test at NEES@UMN (MAST) Specimen 1. Network for Earthquake Engineering Simulation (NEES).

[10]. Gavridou S, Wallace JW, Nagae T, Matsumori T, Tahara K, and Fukuyama K (2017): Shake-Table Test of a Full-Scale 4-Story Precast Concrete Building. II: Analytical Studies. *Journal of Structural Engineering*, **143**(6).

[11]. Priestley MJN, Calvi GM, and Kowalsky MJ (2007): *Displacement-based design of structures*. Pavia: IUSS Press.

[12]. Muir CA, Bull DK, and Pampanin S (2012): Preliminary observations from biaxial testing of a two-storey, two-by-one bay, reinforced concrete slotted beam superassembly. *Bulletin of the New Zealand Society for Earthquake Engineering*, **45**(3): 97-104.

[13]. Lu Y, Gu A, Xiao Y, Henry RS, Elwood KJ, Rodgers G, Zhou Y, and Y. YT (2018). Shake-table test on a low damage concrete wall building: Building design. *The Eleventh U.S. National Conference on Earthquake Engineering*. Los Angeles.

[14]. Sarti F, Palermo A, and Pampanin S (2016): Fuse-Type External Replaceable Dissipaters: Experimental Program and Numerical Modeling. *Journal of Structural Engineering*, **142**(12): 04016134.

[15]. Rodgers GW, Solberg KM, Chase JG, Mander JB, Bradley BA, Dhakal RP, and Li L (2008): Performance of a damage-protected beam-column subassembly utilizing external HF2V energy dissipation devices. *Earthquake Engineering and Structural Dynamics*, **37**(13): 1549-1564.

